Bimolecular chemical reactions on weighted complex networks

Sungchul Kwon, Woosik Choi, and Yup Kim*
Department of Physics and Research Institute of Basic Sciences, Kyung Hee University, Seoul 130-701, Korea
(Received 3 March 2010; revised manuscript received 9 June 2010; published 10 August 2010)

We investigate the kinetics of bimolecular chemical reactions $A+A\rightarrow 0$ and $A+B\rightarrow 0$ on weighted scale-free networks (WSFNs) with degree distribution $P(k)\sim k^{-\gamma}$. On WSFNs, a weight w_{ij} is assigned to the link between node i and j. We consider the symmetric weight given as $w_{ij}=(k_i k_j)^{\mu}$, where k_i and k_j are the degree of node i and j. The hopping probability T_{ij} of a particle from node i to j is then given as $T_{ij}\propto(k_i k_j)^{\mu}$. From a mean-field analysis, we analytically show in the thermodynamic limit that the kinetics of $A+A\rightarrow 0$ and $A+B\rightarrow 0$ are identical and there exist two crossover μ values, $\mu_{1c}=\gamma-2$ and $\mu_{2c}=(\gamma-3)/2$. The density of particles $\rho(t)$ algebraically decays in time t as $t^{-\alpha}$ with $\alpha=1$ for $\mu<\mu_{2c}$ and $\alpha=(\mu+1)/(\gamma-\mu-2)$ for $\mu_{2c}\leq\mu<\mu_{1c}$. For $\mu\geq\mu_{1c}$, ρ decays exponentially. With the mean-field rate equation for $\rho(t)$, we also analytically show that the kinetics on the WSFNs is mapped onto that on unweighted SFNs with $P(k)\sim k^{-\gamma'}$ with $\gamma'=(\mu+\gamma)/(\mu+1)$.

DOI: 10.1103/PhysRevE.82.021108 PACS number(s): 05.40.−a, 82.20.−w, 89.75.Da, 89.75.Hc

I. INTRODUCTION

Irreversible bimolecular chemical reactions $A+A\rightarrow 0$ and $A+B\rightarrow 0$ have attracted continuous interest during last decades because of wide applications to various fields such as physics, chemistry and biology [1–10]. The both reactions instantaneously take place when two reactants encounter on the same site. In higher dimensions than the upper critical dimensions $d\geq d_c$, the kinetics of both reactions follow a classical mean-field rate equation and the density ρ decays in time t as t^{-1}. For $d<d_c$, the kinetics of both reactions are completely different [4]. For $A+A\rightarrow 0$, the reaction leads to the anticorrelation between particles, which results in $\rho\sim t^{-d/2}$ with $d_c=2$ [4,5]. On the other hand, for $A+B\rightarrow 0$, the random fluctuation in the initial particle number of each species plays a crucial role. For homogeneous initial distributions with equal densities of A and B, $\rho_A(0)=\rho_B(0)$, the fluctuations cause the segregation of unlike particles, which drastically slows down the reaction speed by restricting the reaction to occur at the boundaries between segregated domains of unlike particles. As a result, $\rho(t)$ decays as $t^{-d/4}$ with $d_c=4$ [4,6–10]. Subsequent studies showed that the kinetics of $A+B\rightarrow 0$ depends on various physical properties such as the anisotropy of particle motion and the types of interactions between particles such as hard-core and long-ranged attractive interaction [8,11–14].

Critical properties of dynamical phenomena on complex networks have been intensively studied because the interplay between particle interaction and underlying network structure leads to the anomalous behavior distinct from standard mean-field behaviors on regular lattices [15]. On scale-free networks (SFNs) with degree distribution $P(k)\sim k^{-\gamma}$, it was shown that the critical properties of interacting particle systems studied so far strongly depend on γ [15]. In this context, the bimolecular reactions $A+A\rightarrow 0$ and $A+B\rightarrow 0$ have been studied on SFNs [16–20].

Gallos and Argyrakis first studied the reactions $A+A\rightarrow 0$ and $A+B\rightarrow 0$ on SFNs [16]. They numerically showed on SFNs with $2\leq\gamma\leq 3.5$ that ρ decays as $t^{-\alpha}$ for both reactions. However, the decay exponent α is larger than 1 and also continuously varies with γ. From the results, they argued that the anomalous density decay with $\alpha>1$ results from the uniform mixing of reactants and the existence of hub nodes in the networks [16–18]. A systematic mean-field analysis for $A+A\rightarrow 0$ reaction was followed by Catanzaro *et al.* [19]. From the mean-field rate equation for the average density ρ_k of a node with degree k, they showed $\rho\sim t^{-1}$ for $\gamma>3$, $(t\ln t)^{-1}$ for $\gamma=3$, and $t^{-1/(\gamma-2)}$ for $\gamma<3$ in the infinite network limit ($N\rightarrow\infty$). The anomalous decay for $\gamma<3$ results from the fact that most reactions occur at hub nodes through which particles vanish and thus the reaction rate is proportional to the number of hub nodes [19]. However, it was shown that ρ always decays as t^{-1} on finite-sized SFNs with $\gamma>3$ because $\langle k^2\rangle$ is always finite [19]. For $A+B\rightarrow 0$, Weber *et al.* confirmed the same behavior as that of $A+A\rightarrow 0$ [20].

On the other hand, most real-world networks exhibit not only heterogeneous degree distributions, but also heterogeneous distributions of weights [21,22]. Weights assigned on links characterize the interaction strengths between nodes. There have been various attempts to understand the underlying mechanism and scale-free behaviors of empirically observed weighted networks [21–27]. Also there have been attempts to understand the effect of heterogeneous weights on various dynamical processes [15,28–32]. These studies showed that dynamical properties are modified and exhibit nontrivial dependence on the strength of weight.

The weight w_{ij} represents the weight to a link between node i and j. In general, the strength S_i of the node i with degree k_i scales as $S_i\sim k_i^{\mu}$ and μ varies with network structures [24,25]. Thus it is natural to take the weight w_{ij} as $w_{ij}\sim S_i S_j\sim(k_i k_j)^{\mu}$, which was observed in a worldwide airport network and a certain metabolic network [24,26]. On weighted scale-free networks (WSFNs) with symmetric weight $w_{ij}\sim(k_i k_j)^{\mu}$, physical properties of various equilibrium and nonequilibrium systems have been studied [15,28–32]. For Ising model on WSFNs with $P(k)\sim k^{-\gamma}$ and $w_{ij}\sim(k_i k_j)^{\mu}$, it was suggested that the critical behavior on the WSFNs is the same as that on unweighted SFNs with degree

*Corresponding author; ykim@khu.ac.kr

exponent $\gamma'=(\gamma+\mu)/(1+\mu)$ [28]. The mapping relation was tested for several nonequilibrium systems such as contact process [28–31] and it was shown that there are exceptions to the relation [30,31]. Hence, it is also worth identifying that the present reaction systems fulfill the mapping relation.

In this paper, we investigate the kinetics of $A+A\to 0$ and $A+B\to 0$ on WSFNs with $w_{ij}\sim(k_ik_j)^\mu$. We derive the mean-field rate equation for $\rho_k(t)$ and obtain a self-consistent rate equation for total density $\rho(t)$ using quasi-static approximation as in Refs. [19,20]. The structures of the equation of ρ_k for both reactions are identical except numerical prefactors so the kinetics of both reactions are the same. From the equation of ρ, we find in the limit $N\to\infty$ that there exist three distinct scaling regimes divided by two crossover μ values, $\mu_{1c}=\gamma-2$ and $\mu_{2c}=(\gamma-3)/2$, respectively. $\rho(t)$ decays as $t^{-\alpha}$ with $\alpha=1$ for $\mu<\mu_{2c}$ and $\alpha=(\mu+1)/(\gamma-\mu-2)$ for $\mu_{2c}\le\mu<\mu_{1c}$. For $\mu\ge\mu_{1c}$, ρ decays exponentially.

However, for finite-sized networks, the mean-field analysis always predicts $\rho\sim t^{-1}$ for any μ. Since simulations are always preformed on finite-sized networks, we cannot confirm the mean-field predictions for $\mu_{2c}\le\mu<\mu_{1c}$ as in Refs. [19,20]. However, with fixed γ, our simulation results for $\mu_{2c}<\mu<\mu_{1c}$ show that $\rho(t)$ decays as $t^{-\alpha}$ with μ dependent α for $t<\tau_c$ and t^{-1} for $t>\tau_c$, where τ_c is the certain crossover time above which the finite-size effect comes into play. From the mean-field rate equations, we also analytically show that the kinetics on WSFNs is mapped onto that on unweighted SFNs with degree exponent $\gamma'=(\gamma+\mu)/(1+\mu)$.

This paper is organized as follows. We define the reactions on WSFNs and present the mean-field analysis in Sec. II. We present simulation results in Sec. III and summarize our results in Sec. IV.

II. MEAN-FIELD ANALYSIS FOR $A+A\to 0$ AND $A+B\to 0$

We consider $A+A\to 0$ and $A+B\to 0$ on WSFNs with the weight $w_{ij}=(k_ik_j)^\mu$ between node i and j. The connectivity of the network is represented by the adjacency matrix $\mathbf{A}$ whose element $a_{ij}=1$ if there is a link from a node j to i. Otherwise, $a_{ij}=0$. We set $a_{ii}=0$ conventionally. The degree k_i of a node i is given as $k_i=\Sigma_j a_{ji}$. For weighted networks, the hopping probability T_{ji} of a particle from node i to j is then given as $T_{ji}=\omega_{ji}/S_i$, where $S_i=\Sigma_j a_{ji}\omega_{ij}$ is the strength of node i. For the symmetric weight $w_{ij}=(k_ik_j)^\mu$, T_{ji} is then given as $T_{ji}=(k_ik_j)^\mu/S_i$ with $S_i=\Sigma_{\langle m\rangle}(k_ik_m)^\mu$. The sum $\Sigma_{\langle m\rangle}$ denotes the sum over the linked nodes to node i. In what follows, we call the directly linked nodes to node i as the nearest neighbors of node i.

The models for the reactions on the networks are defined as follows. One randomly selects a node i. If the node i is occupied by a particle, then the particle attempts to move to a randomly selected nearest neighbor, say node j, with probability T_{ji}. If the target node j is empty, then the attempt is accepted. Otherwise, for $A+A\to 0$ reaction, the reaction occurs instantaneously and the particles on node i and j annihilate. For $A+B\to 0$, we consider the model with hard-core interaction between like particles. Hence, if the target node is occupied by a like particle, the hopping attempt is rejected. If an unlike particle occupies the target node, then the reaction occurs.

First, we present a mean-field analysis for $A+A\to 0$ reaction. The mean-field rate equation for the density ρ_i of node i is written down as

$$\frac{d\rho_i(t)}{dt}=-\rho_i(t)+\sum_{j=1}^{N}a_{ij}T_{ij}[1-2\rho_i(t)]\rho_j(t). \tag{1}$$

The first term represents the outflow of a particle from node i. The second term consists of the inflow of a particle from node j to i and the annihilation of a particle on node i with an incoming particle from node j. For further analysis, it is easy to consider the average density ρ_k of a node with the degree k defined as

$$\rho_k=\frac{1}{N_k}\sum_{i=1}^{N}\rho_i\delta_{k_ik}=\frac{1}{N_k}\sum_{i\in\Omega(k)}\rho_i. \tag{2}$$

N_k is the number of nodes with degree k and $\delta_{\ell m}$ is Kronecker delta. $\Omega(k)$ denotes the set of nodes with degree k. We neglect the fluctuations of ρ_k for any k and thus approximate $\rho_j=\rho_{k'}$ for $j\in\Omega(k')$. We also approximate $T_{ij}=T_{kk'}$ for $i\in\Omega(k)$ and $j\in\Omega(k')$. $T_{kk'}$ is the hopping probability from a node with degree k' to a node with degree k. From Eqs. (1) and (2), one obtains

$$\frac{d\rho_k(t)}{dt}=-\rho_k+(1-2\rho_k)\sum_{k'}\rho_{k'}T_{kk'}\frac{1}{N_k}\sum_{i\in\Omega(k)}\sum_{j\in\Omega(k')}a_{ij}. \tag{3}$$

The sum $\frac{1}{N_k}\Sigma_{i\in\Omega(k)}\Sigma_{j\in\Omega(k')}a_{ij}$ is the average number of nodes with degree k' linked to a node with degree k, i.e., $kP(k'|k)$ [19]. $P(k'|k)$ is the conditional probability of a node with degree k' being linked to a node with degree k. For uncorrelated networks, $P(k'|k)$ is known to be $P(k'|k)=k'P(k')/\langle k\rangle$ [15]. Then Eq. (3) becomes

$$\frac{d\rho_k(t)}{dt}=-\rho_k+\frac{k(1-2\rho_k)}{\langle k\rangle}\sum_{k'}\rho_{k'}k'P(k')T_{kk'}. \tag{4}$$

For $T_{kk'}=1/k'$, Eq. (4) is reduced to the equation on unweighted SFNs [19]. For the weighted networks, $T_{kk'}$ is given as $T_{kk'}=(kk')^\mu/S_{k'}=k^\mu/\Sigma_{m=1}^{k'}k_m^\mu$ with $S_{k'}=\Sigma_{m=1}^{k'}(k_mk')^\mu$. Since we consider a mean-field approximation, we again neglect the fluctuation of k_m^μ in the sum $\Sigma_{m=1}^{k'}k_m^\mu$ and replace k_m^μ with the averaged k_m^μ over the nodes with degree k', i.e., $\langle k_m^\mu\rangle_{k'}$. Then one gets $\Sigma_{m=1}^{k'}(k_m)^\mu\approx k'\langle k_m^\mu\rangle_{k'}$. The average $\langle k_m^\mu\rangle_{k'}$ is given as $\langle k_m^\mu\rangle_{k'}=\int k_m^\mu P(k_m|k')dk_m$, where $P(k_m|k')$ is the conditional probability of a node with degree k_m being linked to a node with degree k'. With $P(k_m|k')=k_mP(k_m)/\langle k\rangle$, we get $\langle k_m^\mu\rangle_{k'}=\langle k^{1+\mu}\rangle/\langle k\rangle$ and finally $T_{kk'}=k^\mu\langle k\rangle/(k'\langle k^{1+\mu}\rangle)$. With the relation of total density ρ and ρ_k, $\rho=\Sigma_{k=1}^{\infty}\rho_kP(k)$, Eq. (4) becomes

$$\frac{d\rho_k(t)}{dt}=-\rho_k(t)+\frac{k^{1+\mu}[1-2\rho_k(t)]}{\langle k^{1+\mu}\rangle}\rho(t). \tag{5}$$

We can obtain the rate equation for total density $\rho(t)$ by multiplying Eq. (5) by $P(k)$ and summing up over k

$$\frac{d\rho(t)}{dt} = -2\rho(t)\Theta(t), \tag{6}$$

where

$$\Theta(t) = \frac{1}{\langle k^{1+\mu}\rangle}\sum_k k^{1+\mu}\rho_k(t)P(k). \tag{7}$$

To solve Eq. (6), we adopt quasistatic approximation [19]. Since ρ decays in time, $d\rho/dt$ is much smaller than ρ in long-time limit, i.e., $d\rho/dt \ll \rho$ for $t\to\infty$. For the same reason, we have $d\rho_k/dt \ll \rho_k$ and thus set $d\rho_k/dt=0$ in Eq. (5). Then we obtain

$$\rho_k(t) = \frac{k^{1+\mu}\rho(t)/\langle k^{1+\mu}\rangle}{1+2k^{1+\mu}\rho(t)/\langle k^{1+\mu}\rangle}. \tag{8}$$

Substituting ρ_k of Eq. (8) into Eq. (7), we finally obtain the self-consistent rate equation for $\rho(t)$, namely,

$$\frac{d\rho(t)}{dt} = -\frac{2\rho^2(t)}{\langle k^{1+\mu}\rangle^2}\sum_k \frac{k^{2(1+\mu)}P(k)}{1+2k^{1+\mu}\rho(t)/\langle k^{1+\mu}\rangle}. \tag{9}$$

Equation (9) is reduced to that of the unweighted SFNs when $\mu=0$ [19].

Next, we discuss the divergence of $\langle k^{1+\mu}\rangle$ and $\langle k^{2(1+\mu)}\rangle$. First, $\langle k^{1+\mu}\rangle$ is finite for $\mu<\gamma-2$ and diverges for $\mu\geq\gamma-2$. For $\langle k^{1+\mu}\rangle$=finite, one obtains at the lowest order of $\rho(t)$

$$d\rho/dt = -2\langle k^{2(1+\mu)}\rangle\rho^2/\langle k^{1+\mu}\rangle^2. \tag{10}$$

However, $\langle k^{2(1+\mu)}\rangle$ diverges for $\mu\geq(\gamma-3)/2$ and finite otherwise. Hence, one cannot truncate the series of Taylor expansion of Eq. (9) at the lowest order for $\mu\geq(\gamma-3)/2$. Therefore, we have two crossover values of μ, namely,

$$\mu_{1c} = \gamma-2, \quad \mu_{2c} = (\gamma-3)/2, \tag{11}$$

which make three dynamical regimes, i.e., $\mu<\mu_{2c}$, $\mu_{2c}\leq\mu<\mu_{1c}$ and $\mu_{1c}\leq\mu$ respectively. We obtain the scaling behavior of $\rho(t)$ in each regime as follows.

Regime I For $\mu<\mu_{2c}$, both $\langle k^{1+\mu}\rangle$ and $\langle k^{2(1+\mu)}\rangle$ are finite and thus one obtains Eq. (10) by performing Taylor expansion of Eq. (9). As a result, ρ decays as t^{-1}.

Regime II For $\mu\geq\mu_{1c}$, both $\langle k^{1+\mu}\rangle$ and $\langle k^{2(1+\mu)}\rangle$ diverge. In Eq. (5) one can set the second term to zero because $\langle k^{1+\mu}\rangle$ diverges and ρ decays to zero. Hence, ρ_k decays exponentially as $\rho_k=e^{-t}$ for any k. As a result, ρ also decays as e^{-t}.

Regime III For $\mu_{2c}\leq\mu<\mu_{1c}$, $\langle k^{1+\mu}\rangle$ is finite but $\langle k^{2(1+\mu)}\rangle$ diverges. To solve Eq. (9) in this region, we use the following physical argument [19]. In Eq. (8), for any given time τ, $\rho_k(\tau)$ with degree larger than $\{\langle k^{1+\mu}\rangle/\rho(\tau)\}^{1/(1+\mu)}$ is essentially a constant up to time τ. Therefore, for a given time τ, there exists a crossover degree $k_c(\tau)$ defined as

$$k_c(\tau) = \left[\frac{\langle k^{1+\mu}\rangle}{\rho(\tau)}\right]^{1/(1+\mu)}. \tag{12}$$

For $k>k_c$, $\rho_k\approx 1/2$. However, ρ_k with $k<k_c$ decays in time. $k_c(\tau)$ increases as τ increases. If the given network is finite with the network size N, $k_c(\tau)$ eventually approaches to the maximal degree $k_{max}(N)(\simeq N^{1/(\gamma-1)})$.

The origin of $\rho_k\approx 1/2$ with $k>k_c$ in the regime III can qualitatively be understood from the fact that on the WSFNs, the probability P_i of a random walker being on node i with degree k_i in the steady state scales with k_i as $P_i\sim k_i^{1+\mu}$ [32]. Therefore, particles move toward nodes with larger degree for $\mu>-1$, and thus occupy both hub nodes and their nearest neighbors. When a particle on a hub node annihilates with one of the particles on the nearest neighbors, the hub node is quickly occupied by one of the particles on the nearest neighbors due to biased diffusion with T_{ij}. In such a way, hub nodes play as drains through which particles disappear. As a result, the change of ρ at time t should be proportional to the number of nodes with degree larger than $k_c(t)$ as mentioned in Ref. [19]. Hence one can approximate Eq. (9) as

$$\frac{d\rho(t)}{dt} \sim \int_{k_c(t)}^{\infty} P(k)dk. \tag{13}$$

With $P(k)\sim k^{-\gamma}$ and $k_c(t)$ of Eq. (12), one finally obtains from Eq. (13)

$$\rho(t) \sim t^{-\alpha}[\alpha=(1+\mu)/(\gamma-\mu-2)]. \tag{14}$$

In summary, from the mean-field analysis for $A+A\to 0$ on infinite-sized WSFNs with symmetric weight $w_{ij}\sim(k_ik_j)^{\mu}$, we find that $\rho(t)$ decays as

$$\rho(t) \sim \begin{cases} t^{-1} & \text{for } \mu<(\gamma-3)/2, \\ t^{-\frac{(1+\mu)}{(\gamma-\mu-2)}} & \text{for } (\gamma-3)/2\leq\mu<(\gamma-2), \\ e^{-t} & \text{for } \mu\geq(\gamma-2). \end{cases} \tag{15}$$

However, for finite-sized networks, since all the moments are finite for any μ and γ, Taylor expansion of Eq. (9) is always legitimate. Hence, ρ always decays as $\rho\sim t^{-1}$ for finite-sized networks in the limit $t\to\infty$.

Next, we discuss $A+B\to 0$ reaction, which was studied by Weber *et al.* [20] on unweighted SFNs. With equal densities of A and B, i.e., $\rho_A(0)=\rho_B(0)$, we have $\rho_A(t)=\rho_B(t)$ and thus $\rho(t)=2\rho_A(t)$. The mean-field rate equation for A-particles of a node i, ρ_{Ai}, becomes

$$\frac{d\rho_{Ai}(t)}{dt} = -\rho_{Ai} + \sum_{j=1}^{N} a_{ij}T_{ij}[(1-\rho_i)\rho_{Aj} - \rho_{Ai}\rho_{Bj}]. \tag{16}$$

The average density of each species of particles on a node with degree k is defined as

$$\rho_{Ak} = \frac{1}{N_k}\sum_{i\in\Omega(k)}\rho_{Ai}, \quad \rho_{Bk} = \frac{1}{N_k}\sum_{i\in\Omega(k)}\rho_{Bi}. \tag{17}$$

Following the same steps in $A+A\to 0$, one can obtain the rate equation for ρ_{Ak} from Eq. (16) as

$$\frac{d\rho_{Ak}}{dt} = -\rho_{Ak} + \frac{k}{\langle k\rangle}\sum_{k'}[(1-\rho_k)\rho_{Ak'} - \rho_{Ak}\rho_{Bk'}]k'T_{kk'}P(k'). \tag{18}$$

For $\rho_A(0)=\rho_B(0)$, we approximate $\rho_{Ak}=\rho_{Bk}$ and thus $\rho_k=2\rho_{Ak}=2\rho_{Bk}$. Then from Eq. (18), we obtain the equation for ρ_k as

$$\frac{d\rho_k(t)}{dt} = -\rho_k + \frac{k\left(1-\frac{3}{2}\rho_k\right)}{\langle k\rangle}\sum_{k'}\rho_{k'}k'T_{kk'}P(k'). \quad (19)$$

With $\rho=\Sigma_k\rho_kP(k)$, one obtains for $A+B\to 0$

$$\frac{d\rho(t)}{dt} = -\frac{3}{2}\rho(t)\Theta(t), \quad (20)$$

where

$$\Theta(t) = \frac{1}{\langle k^{1+\mu}\rangle}\sum_k k^{1+\mu}\rho_k(t)P(k). \quad (21)$$

With $T_{kk'}=1/k'$ for $\mu=0$, Eq. (19) of ρ_k is reduce to that of Ref. [20]. On unweighted SFNs ($\mu=0$), Weber *et al.* studied $A+B\to 0$ with hard-core interaction between like particle [20]. They analytically showed that the equation of ρ_k, i.e., Equation (19) with $T_{kk'}=1/k'$, additionally includes the pair-correlation between like particles. However, the correlation decreases in low-density limit, so one can neglect the pair-correlation by the hard-core interaction [20]. Therefore, Eq. (19) is valid in long-time limit on both unweighted and weighted SFNs. Compared with Eqs. (4) and (6) for $A+A\to 0$, the differences in Eqs. (19) and (20) are only the prefactor of ρ_k in the second term in Eq. (19) and of ρ in Eq. (20). Therefore, the structures of the equations for ρ_k and ρ are identical for both reactions. As a result, $A+B\to 0$ reaction exhibits the same kinetics as that of Eq. (15) for $A+A\to 0$ on weighted SFNs as well. We showed that the structure of equation of ρ_k for $A+B\to 0$ is identical to that for $A+A\to 0$ and thus both reactions exhibit the same scaling behavior [20].

Finally, we discuss the mapping of results on WSFNs onto those on unweighted SFNs. We define q as $q=k^{1+\mu}$ and degree distribution $P(q)$ with new exponent γ'. Right hand side of Eq. (9) is written as an integral form for continuous k as

$$\frac{d\rho(t)}{dt} = -\frac{2\rho^2(t)}{\langle k^{1+\mu}\rangle^2}\int^{\infty}\frac{k^{2(1+\mu)}P(k)dk}{1+2k^{1+\mu}\rho(t)/\langle k^{1+\mu}\rangle}. \quad (22)$$

Changing variable k with q, one easily obtains the equation for ρ on unweighted SFNs. From $dq=(1+\mu)k^{\mu}dk$ and $P(k)=\mathcal{N}k^{-\gamma}$ with a normalization factor $\mathcal{N}$, one obtains $P(q)=\mathcal{N}q^{-\gamma'}/(1+\mu)$ satisfying $P(k)dk=P(q)dq$ with

$$\gamma' = \frac{\gamma+\mu}{1+\mu}. \quad (23)$$

Then changing variable with q in Eq. (22), one reads

$$\frac{d\rho(t)}{dt} = -\frac{2\rho^2(t)}{\langle q\rangle^2}\int^{\infty}\frac{q^2P(q)}{1+2q\rho(t)/\langle q\rangle}dq, \quad (24)$$

which is the equation for ρ on unweighted SFNs with $P(q)\sim q^{-\gamma'}$. The crossover μ_{2c} and μ_{2c} of Eq. (11) are then transformed to $\gamma'=2$ and $\gamma'=3$ respectively. The decay exponent $\alpha=(1+\mu)/(\gamma-2-\mu)$ for $\mu_{2c}\le\mu<\mu_{1c}$ becomes $1/(\gamma'-2)$ for $2<\gamma'\le 3$. Therefore, the kinetics of the bimolecular reactions on the WSFNs are exactly mapped onto those on unweighted SFNs with the degree exponent Eq. (23). Hence, we analytically confirm that the bimolecular reaction $A+A\to 0$ and $A+B\to 0$ also satisfy the mapping relation Eq. (23) suggested in Ref. [28].

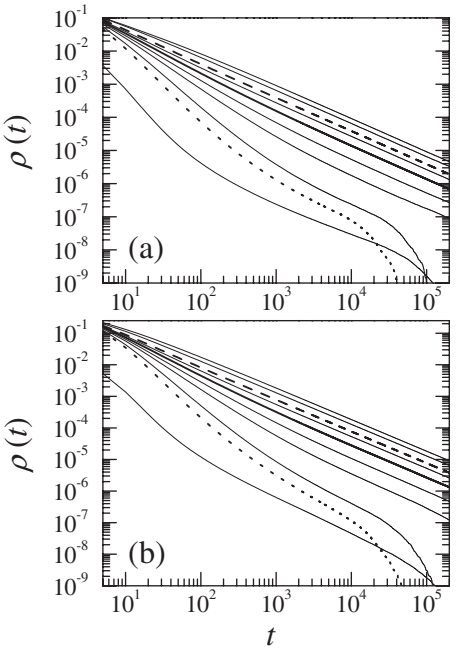

FIG. 1. The plot of $\rho(t)$ for $\gamma=4$: (a) ρ for $A+A\to 0$ and (b) ρ_A for $A+B\to 0$. In each panel, from top to bottom, each line corresponds to $\mu=-2,-1$, 0 (dashed), 0.25, 0.5 (thick), 0.75, 1, 1.5, 2 (dotted), and 3, respectively. For clarity, we shift the data line for $\mu=3$ by multiplying the data by 0.1 for $A+A$ and 0.05 for $A+B$. For $\gamma=4$, $\mu_{2c}=0.5$ and $\mu_{1c}=2.0$.

III. MONTE CARLO SIMULATIONS

To confirm the mean-field prediction of Eq. (15), we perform Monte Carlo simulations on the WSFNs. For the construction of WSFNs, we first construct an unweighted static SFNs with N nodes and K links with $\langle k\rangle=2K/N$ [33]. After then, we assign a symmetric weight $w_{ij}=(k_ik_j)^{\mu}$ to the link between node i and j. We simulate the bimolecular reactions on the WSFNs with $\gamma=4$ and 2.5, $N=10^7$ and $\langle k\rangle=8$. From Eq. (11), one reads $\mu_{1c}=2$ and $\mu_{2c}=0.5$ for $\gamma=4$, and $\mu_{1c}=0.5$ and $\mu_{2c}=-0.25$ for $\gamma=2.5$, respectively. We run simulations up to 2×10^5 Monte Carlo steps and average $\rho(t)$ over 2000 independent runs for various μ.

First, we discuss the kinetics of both reactions for $\gamma=4$. Figure 1 shows the double logarithmic plot of $\rho(t)$ for both reactions against t for various μ from -2 to 3. For the comparison, we also plot $\rho(t)$ of $\mu=0$ (dashed line). As expected by the mean-field analysis, the kinetics of $A+B$ is the same as that of $A+A$. For $\mu\le 0.5$ (regime I), the mean-field analysis predicts $\rho(t)\sim t^{-1}$. We estimate the decay exponent α from the scaling plot of ρt^{α} against t. For $\mu\le 0.5$, we estimate $\alpha=1.0(1)$ which agrees well with the mean-field prediction of Eq. (15) for $\mu\le\mu_{2c}$. On the other hand, since $\rho(t)$ decays as $(t\ln t)^{-1}$ on unweighted SFNs with $\gamma=3$ [19,20], we also expect the logarithmic correction for $\mu=\mu_{2c}$ which corresponds to unweighted SFNs with $\gamma=3$.

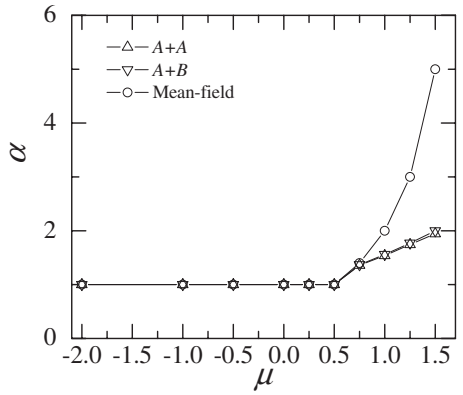

FIG. 2. The plot of α against μ for $\gamma=4$: Triangles denote the estimated α obtained from the scaling plot ρt^{α} for $A+A\to 0$ (up-triangles) and $A+B\to 0$ (down-triangles). Circles denote the mean-field α_{MF} of Eq. (15). The line between data is a guide to the eye. For $\gamma=4$, $\mu_{2c}=0.5$ and $\mu_{1c}=2.0$. The estimates of α for $\mu>0.5$ are obtained from $\rho(t)$ with $t<\tau_c$.

For $0.5<\mu<2$ (regime III), the mean-field analysis predicts $\rho\sim t^{-\alpha}$ with $\alpha=(1+\mu)/(\gamma-\mu-2)$ for $N\to\infty$. However, since we deal with finite-sized networks with a finite maximal degree k_{max} in simulations, all moments of degree are finite as well. From Eqs. (10) and (20), $\rho(t)$ decays on finite-sized networks as

$$\rho(t)\sim\frac{\langle k^{1+\mu}\rangle^2}{\langle k^{2(1+\mu)}\rangle}t^{-1} \tag{25}$$

regardless of μ values for both reactions. However, for $\mu_{2c}<\mu<\mu_{1c}$, there exists a crossover time τ_c. The effect of finite k_{max} comes into play for $t>\tau_c$. For $t<\tau_c$, particles do not feel the finite-sized effect yet, so $\rho(t)$ tends to follow the mean-field behavior of Eq. (15) for both reactions. As a result, $\rho(t)$ is expected to undergo the crossover from the mean-field behavior of Eq. (15) for $t<\tau_c$ to the t^{-1} decay of Eq. (25) for $t>\tau_c$. One can estimate τ_c for static networks with $k_{max}\sim N^{-1/(\gamma-1)}$ using Eq. (12). Since the crossover degree $k_c(t)$ increases in time to k_{max}, the finite-size effect comes into play when $k_c(\tau_c)=k_{max}$. With $\rho(\tau_c)\sim\tau_c^{-\alpha}$ and $k_c(\tau_c)=k_{max}$, one finds for $\mu_{2c}<\mu<\mu_{1c}$

$$\tau_c\sim N^{(\gamma-2-\mu)/(\gamma-1)}, \tag{26}$$

where $(\gamma-2-\mu)/(\gamma-1)<1$ for $\mu>-1$.

We estimate the exponent α assuming $\rho(t)\sim t^{-\alpha}$ for $t<\tau_c$ from the scaling plot. In Fig. 2. we plot the estimated α of both reactions together with the mean-field α (α_{MF}) of Eq. (15). As shown, the difference between α and α_{MF} becomes larger as μ increases. It comes from the fact that τ_c decreases with μ and thus we should measure α in the shorter initial time interval $t<\tau_c$ for the larger μ. As a result, it is practically hard to confirm the mean-field scaling behavior of Eq. (15) due to the strong finite-size effect.

To confirm Eq. (26), we measure τ_c of $A+A\to 0$ reaction for $\mu=0.75$. we estimate $\alpha=1.36(1)$ from the scaling plot for $t<\tau_c$, which is close to $\alpha_{MF}=1.4$. First, we find time intervals in which $\alpha=1.36$ and 1.0 by the scaling plot. Then, we obtain the fitting line of $\rho(t)$ in each time interval and estimate τ_c by using the intersection of the two fitting lines. In such a way, we obtain τ_c for several N up to 10^7. Figure 3 shows the double logarithmic plot of τ_c against N for $\mu=0.75$. As shown, simulation results agree well with the theoretical line with slope $(\gamma-2-\mu)/(\gamma-1)=0.416$ for $\gamma=4$.

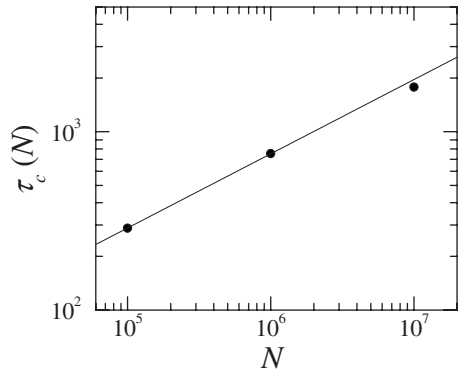

FIG. 3. The plot of τ_c for $\mu=0.75$. The symbols denote simulation data. The line corresponds to the theoretical line with slop $(\gamma-2-\mu)/(\gamma-1)=0.416$ for $\gamma=4$.

For $\mu\geq 2$ (regime II), one can neglect the second term in Eq. (5) on infinite-sized networks and thus expects $\rho(t)=e^{-t}$. However, on finite-sized networks, $\rho(t)$ always decays as t^{-1} in long time limit. Therefore, one expects the crossover from $\rho=e^{-t}$ for $t<\tau_c$ to t^{-1} for $t>\tau_c$ on finite-sized networks. τ_c is a crossover time above which the finite-size effect comes into play. In Fig. 1, we plot $\rho(t)$ for $\mu=3$ for both reactions. $\rho(t)$ begins to decay as t^{-1} in very early time. It means that τ_c is very small for $\mu\geq 2$. Due to very small τ_c, we cannot numerically confirm $\rho(t)=e^{-t}$ for $t<\tau_c$. To estimate τ_c for $\mu\geq 2$, one should take into account N dependence of $\langle k^{1+\mu}\rangle$ because $\langle k^{1+\mu}\rangle$ diverges for $\mu\geq 2$. With $\langle k^{1+\mu}\rangle\sim k_{max}^{2+\mu-\gamma}$ and $\rho(t)=e^{-t}$, one finds $\tau_c\sim\ln N$ for $\mu\geq 2$. As a result, τ_c logarithmically increases with N for $\mu\geq 2$, so it is practically impossible to numerically confirm the mean-field prediction.

Next, we discuss the kinetics on SFNs with $\gamma=2.5$ where $\mu_{1c}=0.5$ and $\mu_{2c}=-0.25$. In Fig. 4, we plot $\rho(t)$ of both reactions for various μ from -2 to 1.5. Except $\mu=-2$ and 1.5, the time dependency of $\rho(t)$s is similar to that of $\gamma=4$ as expected by the mean-field analysis. $\rho(t)$ decays as t^{-1} in regime I ($\mu\leq -0.25$). In regime III ($-0.25<\mu<0.5$), $\rho(t)$ decays as $t^{-\alpha}$ with μ dependent α for $t<\tau_c$ and decays as t^{-1} for $t>\tau_c$. In Fig. 5, we plot the estimated α from the scaling plot. The behavior of α is similar to that of $\gamma=4$. However, for $\mu=-2$, $\rho(t)$ slowly decays with continuously decreasing exponent for both reactions. It means that $\rho(t)$ saturates to a certain value in long-time limit (Fig. 6). It can be understood from the fact that as $\mu\to-\infty$, particles are trapped on nodes with one edge, i.e., dangling nodes. As a result, trapped particles are hard to react with each other, which results in the saturation of $\rho(t)$ for $\mu\to-\infty$. One can see this tendency more clearly for $A+B\to 0$ than $A+A\to 0$ because of the anticorrelation between unlike particles. On the other hand, for $\mu=1.5$, $\rho(t)$ undergoes an exponential decay without the t^{-1}-decay behavior. It means that τ_c and the time needed to visit the whole nodes in a network are the same order for $N=10^7$. Hence, to observe the t^{-1} decay, we need more big sized networks with $N\gg 10^7$.

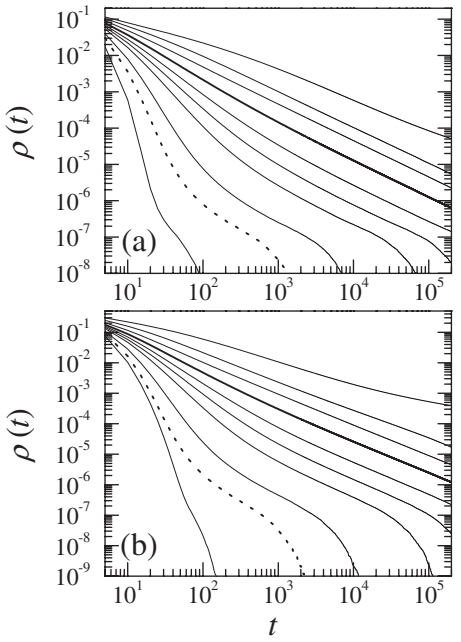

FIG. 4. The plot of $\rho(t)$ for $\gamma=2.5$: (a) ρ for $A+A\to 0$ and (b) ρ_A for $A+B\to 0$. In each panel, from top to bottom, each line corresponds to $\mu=-2,-1,-0.5,-0.25$(thick),-0.1, 0.0, 0.1, 0.3, 0.5 (dashed), and 1.5, respectively. For $\gamma=2.5$, $\mu_{2c}=-0.25$, and $\mu_{1c}=0.5$.

Finally we numerically examine the validity of the quasistatic approximation of Sec. II. The main nontrivial result of the mean-field analysis in Sec. II is the existence of the regime III. The most important consequence in the regime III is Eq. (8) which mainly governs most dynamical features of the bimolecular reactions. The important consequence of Eq. (8) is the existence of the crossover degree k_c of Eq. (12) at any given time t. As a result, ρ_k with $k \gg k_c(t)$ at a given time t remains as a constant (or 1/2). However, for $k \ll k_c(t)$, ρ_k scales as $t^{-\alpha}k^{1+\mu}$. In addition, Eq. (8) shows that ρ_k is a function of one scaling variable k/k_c. Hence, ρ_k in the regime III is simply written as

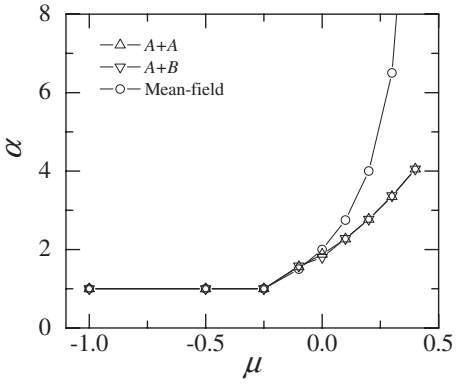

FIG. 5. The plot of α against μ for $\gamma=2.5$: Triangles denote the estimated α for $A+A\to 0$ (up-triangles) and $A+B\to 0$ (down-triangles). Circles denote the mean-field α_{MF} of Eq. (15). The line between data is a guide to the eye. For $\gamma=2.5$, $\mu_{2c}=-0.25$ and $\mu_{1c}=0.5$. The estimates of α for $\mu>-0.25$ are obtained from $\rho(t)$ with $t<\tau_c$.

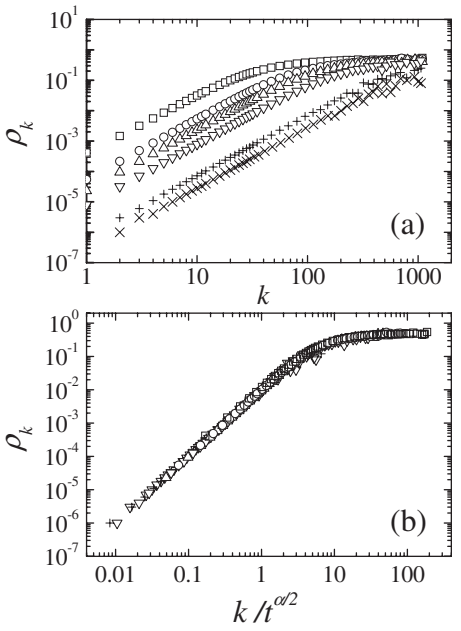

FIG. 6. The plot of ρ_k and the scaling collapse with $\mu=1$. (a) ρ_k for $t=10$, 30,,50,,100,,500, and 1000 from top to bottom. (b) the scaling collapse of ρ_k against $kt^{-\alpha/2}$.

$$\rho_k(t) = F(k/k_c) = G(kt^{-\alpha/(1+\mu)}). \tag{27}$$

The scaling function $G(x)$ approaches to 1/2 for $x \gg 1$ and scales as $x^{1+\mu}$ for $x \ll 1$. Therefore, the validity of the quasistatic approximation can be confirmed by examining the scaling relation of Eq. (27). Equation (27) also provides another way to estimate α of the regime III in addition to the scaling plot of ρt^{α}.

We measure $\rho_k(t)$ up to $t=10^3$ for $\mu=1$ and $\gamma=4$, which belongs to the regime III. The results are plotted in Fig. 6(a). As shown, ρ_k for $t<500$ increases with k in power-law and saturates to 1/2 as expected by Eq. (8). Hence, in this time interval, the finite-size effect does not come into play yet. For $t \geq 500$, however, ρ_k algebraically increases without the saturation, which means that k_c already reaches to k_{max}. We confirm $\rho_k \sim k^2$ for $k<k_c$ at all times as expected. To confirm Eq. (27), we plot ρ_k of various times against $kt^{-\alpha/(1+\mu)}$ by varying α [Fig. 6(b)]. We obtain the best scaling collapse of the data to Eq. (27) with $\alpha=1.54(2)$. $\alpha=1.54$ is the same as that obtained from the scaling plot ρt^{α} for $t<\tau_c$ in Fig. 2. Therefore, we numerically confirm that the quasi-static approximation is valid and thus Eq. (8) correctly describes the behavior of ρ_k.

IV. SUMMARY

In summary, we investigate the kinetics of bimolecular reaction $A+A\to 0$ and $A+B\to 0$ on weighted scale-free networks (WSFNs) with degree distribution $P(k)\sim k^{-\gamma}$ and symmetric weight $\omega_{ij}\sim(k_i k_j)^{\mu}$. In the model, a particle moves from node i to one of the nearest neighboring node, say node j with probability $T_{ij}\sim(k_i k_j)^{\mu}$. The reaction occurs instantaneously when two reactants encounter on the same node. From the mean-field analysis for infinite size networks,

we derive the self-consistent rate equation for density $\rho(t)$, which is identical in both reactions except a numerical prefactor. Therefore, the kinetics of both reactions are the same.

From the equation of $\rho(t)$, we show that there exist two crossover values of μ given by $\mu_{1c}=\gamma-2$ and $\mu_{2c}=(\gamma-3)/2$ for a given γ, which divide μ axis into three regimes, i.e., $\mu<\mu_{2c}$, $\mu_{2c}\leq\mu<\mu_{1c}$, and $\mu\geq\mu_{1c}$. $\rho(t)$ decays in time t as t^{-1} for $\mu<\mu_{2c}$ and $t^{-\alpha}$ with $\alpha=(1+\mu)/(\gamma-2-\mu)$ for $\mu_{2c}\leq\mu<\mu_{1c}$. For $\mu\geq\mu_{1c}$, $\rho(t)$ decays exponentially. We also analytically show that the equation of $\rho(t)$ on the WSFNs is exactly mapped onto that on unweighted SFNs with new degree exponent $\gamma'=(\gamma+\mu)/(1+\mu)$. Hence, we analytically confirm the mapping relation suggested in Ref. [28] for both reactions.

We perform Monte Carlo simulations on the WSFNs of the size $N=10^7$ with $\gamma=4$ and 2.5 for both reactions and confirm that the kinetics of both reactions are identical. However, on finite-sized networks, we always observe $\rho(t)\sim t^{-1}$ in long time limit for any μ due to finite maximal degree k_{max} as predicted by the mean-field analysis. For $\mu\leq\mu_{2c}$, we numerically confirm the mean-field prediction of $\rho(t)\sim t^{-1}$. However, for $\mu_{2c}<\mu<\mu_{1c}$, $\rho(t)$ decays as $t^{-\alpha}$ with μ dependent α for $t<\tau_c$ and t^{-1} for $t>\tau_c$, where τ_c is the crossover time above which the finite-size effect comes into play. Hence, for $t<\tau_c$, particles do not feel the finite-sized effect yet, so $\rho(t)$ tends to follow the mean-field behavior. However, our estimates of α are smaller than the mean-field exponent α_{MF}. The difference between our estimate and α_{MF} becomes larger as μ increases. It comes from the fact that τ_c decreases with μ as $\tau_c\sim N^{(\gamma-2-\mu)/(\gamma-1)}$.

For $\mu\geq\mu_{1c}$, the mean-field analysis predicts $\rho(t)\sim e^{-t}$. However in simulations, we have seen a crossover to t^{-1} at very early time for $\gamma=4$ and cannot confirm the mean-field behavior. For $\mu\geq\mu_{1c}$, τ_c is expected to scale as $\tau_c\sim\ln N$, which is too small to confirm the exponential decay. As a result, on finite-sized networks, it is practically impossible to numerically confirm the mean-field predictions for the bimolecular reactions because τ_c increases very slowly with N.

Finally, we propose the scaling relation for ρ_k which is the consequence of the quasi-static approximation used in the mean-field analysis. Through the scaling collapse, we numerically show that $\rho_k(t)$ satisfies the scaling relation of Eq. (27). As a result, the quasi-static approximation is valid and thus the mean-field analysis correctively describes the kinetics of the bimolecular reactions, $A+A\to 0$ and $A+B\to 0$ on both unweighted and weighted SFNs.

In the present paper, we perform simulations on quenched SFNs where links are fixed permanently in time once they are formed. On the other hand, in the heterogeneous mean-field theory in Sec. II, we derive the rate equation of ρ_k from the equation of ρ_i by approximating T_{ij} to $T_{kk'}$. It means that a particle on a node with degree k can move to any nodes with degree k' according to the hopping probability $T_{kk'}$. In annealed networks, links are not fixed in contrast to quenched networks. At each time step, a node with degree k chooses k neighbors randomly according to the degree distribution. Therefore, the mean-field theory is expected to be exact in annealed networks. Recent study on random walks on weighted annealed networks showed that the simulation results on the annealed networks agree with a heterogeneous mean-field theory [34]. For the bimolecular reactions, one may also expect a good agreement between simulation results and the mean-field predictions on such annealed networks. However, the difference between the mean-field theory and simulation comes from the finite maximal degree k_{max}. Furthermore, the mean-field theory predicts that the crossover time τ_c decreases with μ, which makes estimate of the exponent α more imprecise for larger μ. As a result, simulation results on annealed networks are also expected to exhibit the same tendency as that on quenched networks. However, in annealed networks, when k_{max} scales with network size N as $N^{1/\omega}$ with $\omega>\gamma-1$, the finite-size scaling theory for an certain nonequilibrium absorbing phase transition, e.g., contact process, is known to modified by ω [35]. In this sense, it is also interesting to study the kinetics of the bimolecular reactions on annealed networks.

ACKNOWLEDGMENTS

This work was supported by a grant from the Kyung Hee University (Grant No. KHU-20100129), by the Mid-career Research Program through NRF grant (MEST) (Grant No. 2007-0052659) and by the Korea Research Foundation Grant funded by the Korean Government (MOEHRD, Basic Research Promotion Fund) (Grant No. KRF-2007-313-C00279)

[1] N. G. van Kampen, *Stochastic Processes in Physics and Chemistry* (North-Holland, Amsterdam, 1981).
[2] P. G. de Gennes, J. Chem. Phys. **76**, 3316 (1982).
[3] V. Privman, *Nonequilibrium Statistical Mechanics in One Dimension* (Cambridge University Press, Cambridge, England, 1997).
[4] U. C. Täuber, M. Howard, and B. P. Lee, J. Phys. A **38**, R79 (2005).
[5] B. P. Lee, J. Phys. A **27**, 2633 (1994).
[6] A. A. Ovchinnikov and Ya. B. Zeldovich, Chem. Phys. **28**, 215 (1978).
[7] D. Toussaint and F. Wilczek, J. Chem. Phys. **78**, 2642 (1983).
[8] K. Kang and S. Redner, Phys. Rev. Lett. **52**, 955 (1984); K. Kang and S. Redner, Phys. Rev. A **32**, 435 (1985).
[9] M. Bramson and J. L. Lebowitz, Phys. Rev. Lett. **61**, 2397 (1988).
[10] B. P. Lee and J. Cardy, J. Stat. Phys. **80**, 971 (1995).
[11] S. A. Janowsky, Phys. Rev. E **51**, 1858 (1995).
[12] I. Ispolatov, P. L. Krapivsky, and S. Redner, Phys. Rev. E **52**, 2540 (1995).
[13] S. Kwon and Y. Kim, Phys. Rev. E **75**, 021122 (2007).
[14] S. Kwon, S. Y. Yoon, and Y. Kim, Phys. Rev. E **73**, 025102(R) (2006); **74**, 021109 (2006).
[15] S. N. Dorogovtsev and A. V. Goltsev, Rev. Mod. Phys. **80**,

1275 (2008).
[16] L. K. Gallos and P. Argyrakis, Phys. Rev. Lett. **92**, 138301 (2004).
[17] L. K. Gallos and P. Argyrakis, Phys. Rev. E **72**, 017101 (2005).
[18] L. K. Gallos and P. Argyrakis, Phys. Rev. E **74**, 056107 (2006).
[19] M. Catanzaro, M. Boguñá, and R. Pastor-Satorras, Phys. Rev. E **71**, 056104 (2005).
[20] S. Weber and M. Porto, Phys. Rev. E **74**, 046108 (2006).
[21] S. L. Pimm, *Food Webs*, 2nd ed. (University of Chicago Press, Chicago, 2002); Nature (London) **426**, 282 (2003).
[22] R. Albert and A.-L. Barabaśi, Rev. Mod. Phys. **74**, 47 (2002).
[23] S. H. Yook, H. Jeong, A.-L. Barabasi, and Y. Tu, Phys. Rev. Lett. **86**, 5835 (2001).
[24] A. Barrat, M. Barthélemy, R. Pastor-Santorras, and A. Vespignani, Proc. Natl. Acad. Sci. U.S.A. **101**, 3747 (2004).
[25] A. Barrat, M. Barthelemy, and A. Vespignani, Phys. Rev. Lett. **92**, 228701 (2004).
[26] P. J. Macdonald, E. Almaas, and A.-L. Barabási, EPL **72**, 308 (2005).
[27] K.-I. Goh, B. Kahng, and D. Kim, Phys. Rev. E **72**, 017103 (2005).
[28] C. V. Giuraniuc, J. P. L. Hatchett, J. O. Indekeu, M. Leone, I. Perez Castillo, B. Van Schaeybroeck, and C. Vanderzande, Phys. Rev. Lett. **95**, 098701 (2005).
[29] M. Karsai, R. Juhász, and F. Iglói, Phys. Rev. E **73**, 036116 (2006).
[30] Z. Dezsö and A.-L. Barabási, Phys. Rev. E **65**, 055103(R) (2002).
[31] K.-I. Goh, D.-S. Lee, B. Kahng, and D. Kim, Physica A **346**, 93 (2005).
[32] S. Kwon, S. Yoon, and Y. Kim, Phys. Rev. E **77**, 066105 (2008).
[33] K.-I. Goh, B. Kahng, and D. Kim, Phys. Rev. Lett. **87**, 278701 (2001).
[34] A. Baronchelli and R. Pastor-Satorras, Phys. Rev. E **82**, 011111 (2010).
[35] C. Castellano and R. Pastor-Satorras, Phys. Rev. Lett. **100**, 148701 (2008); J. D. Noh and H. Park, Phys. Rev. E **79**, 056115 (2009).